Molecular electronic model and vibronic coupling to ε-vibrational modes of the fluorescent level $^4T_1$ of d^5 ions in II-VI and III-V compounds

D. Boulanger
Université de Paris Sud, Laboratoire d'informatique, Maîtrise de Sciences Physiques, Bâtiment 479, 91405 Orsay Cedex, France

R. Parrot
Institut Universitaire de Formation des Maîtres et Faculté de Technologie de la Guyane, BP 792, 97337 Cayenne Cedex, French Guiana
(Received 27 June 2002; published 12 November 2002)

Complete electronic and vibronic models including the second-order molecular spin-orbit (MSO) interaction are proposed to analyze the fine structure of the orbital triplet levels $^4T_1(G)$ of d^5 ions in tetrahedral symmetry. First, a molecular model which has been used to calculate the first-order MSO interaction is extended to the calculation of the second-order MSO interaction. Then Ham's model for the vibronic coupling to ε-vibrational modes of the first- and second-order MSO interactions is used to describe the fine structure patterns and, in particular, the energy-level ordering in terms of the Huang-Rhys factor *S*. Third, these models are applied to the calculation of the electronic and vibronic structures of the fluorescent level $^4T_1(G)$ of Mn^{2+} in cubic ZnS and in ZnSe. For the level $^4T_1(G)$ of Mn^{2+} in cubic ZnS, the second-order MSO interaction becomes preponderant because the first-order MSO interaction due to the cation can be completely compensated for by the first-order MSO interaction due to the ligands. For the level $^4T_1(G)$ of Mn^{2+} in ZnSe, the first-order MSO interaction is primarily controlled by the ligands. It is shown that the experimental fine structures can be correctly accounted for by the molecular model. Finally, a qualitative model is proposed for the fine structure of the fluorescent level of Fe^{3+} in InP and GaAs.

DOI: 10.1103/PhysRevB.66.205201 PACS number(s): 71.55.Eq, 71.55.Gs, 71.70.Ch, 71.70.Ej

I. INTRODUCTION

Several experimental and/or theoretical studies have been reported concerning the electronic and vibronic fine structure of the fluorescent levels $^4T_1(G)$ of d^5 ions as Mn^{2+} and Fe^{3+} in various II-VI and III-V compounds.[1–11] [The notation $^4T_1(G)$ indicates that in the absence of a crystal field, the level becomes a ^4G level of the free ion.] For example, the fine structure of the fluorescent level has been studied in ZnS:Mn^{2+} and ZnSe:Mn^{2+},[1] GaP:Mn^{2+},[2] ZnS:Fe^{3+},[3] ZnO:Fe^{3+},[4] GaAs:Fe^{3+},[5–7] GaN:Fe^{3+},[8] and InP:Fe^{3+}.[7,9]

We will consider fluorescent levels of tetrahedral symmetry coupled to ε-vibrational modes only. In cubic symmetry, the symmetry of the vibrational modes is deduced from uniaxial stress experiments for applied pressures $\mathbf{P}\|[100]$, $\mathbf{P}\|[1\bar{1}0]$, and $\mathbf{P}\|[111]$. For the fluorescent levels of Mn^{2+} in ZnS and ZnSe,[1] and Fe^{3+} in GaAs and InP (Ref. 7) studied here, the uniaxial stress experiments have unambiguously shown a coupling to *E* strains and therefore to ε-vibrational modes only.

In the following, the crystal field (CF) model is treated as a particular case of the molecular model by restricting the wave functions to those of the *d* electrons of the cation.

The CF model[10] has long been used to analyze the vibronic structure of the level $^4T_1(G)$ in terms of the Huang-Rhys factor *S*. For example, in early studies, the Jahn-Teller effect on the fine structure lines of the fluorescent level of Mn^{2+} in ZnS, ZnSe,[1] and GaP (Ref. 2) was determined from uniaxial stress experiments and interpreted from the CF model by considering a strong coupling to ε-vibrational modes. The fine structures predicted by the CF model are shown in Fig. 1(a). This figure gives the level ordering, in terms of the Huang-Rhys factor *S*, of the four fine-structure lines Γ_6, Γ_7, $\Gamma_8(3/2)$, and $\Gamma_8(5/2)$ of the fluorescent levels of Mn^{2+} in cubic ZnS. The first- and second-order spin-orbit interaction restricted to the electrons *d* of the configuration d^5 have been considered. This figure shows that the level Γ_6 is at lower energy for small values for the Huang-Rhys factor *S* and that the level $\Gamma_8(\frac{3}{2})$ is at lower energy for medium or large values for *S*. However, it was recently shown that, at least in some cases, as Mn^{2+} in cubic ZnS (Refs. 11 and 12) and Fe^{3+} in GaAs and InP,[7] the CF model cannot account for the experimental results in particular for the level ordering of the vibronic lines.

More precisely, in the case of Mn^{2+} in cubic ZnS, uniaxial stress experiments, Zeeman experiments, and an analysis of the relative amplitudes of the fine-structure lines [that is, of the relative dipole strengths (RDS's)] have shown that the level ordering of the fine-structure lines, for increasing energy, is: Γ_7, $\Gamma_8(\frac{3}{2})$, $\Gamma_8(\frac{5}{2})$, and Γ_6. The level Γ_7 being at lower energy, and the level Γ_6 being at higher energy, it is clear that the CF model represented in Fig. 1(a) cannot account for the level ordering of the lines whatever the value for *S* is.

In the case of Fe^{3+} in InP, Zeeman experiments and uniaxial stress experiments performed on emission spectra have shown that the two lines observed at lower energy must be associated to levels Γ_7 and Γ_8 (the level Γ_7 being at lower energy) and that the coupling is to ε-vibrational modes only.[7] For Fe^{3+} in GaAs, Zeeman and uniaxial stress experiments performed on the line at lower energy have shown that the fine structure is similar to that of Fe^{3+} in InP.[7] In these cases, again, the CF model cannot account for the experimental fine structures.

In the case of Mn^{2+} in ZnS and ZnSe, a molecular model has been elaborated which, very surprisingly, showed that the

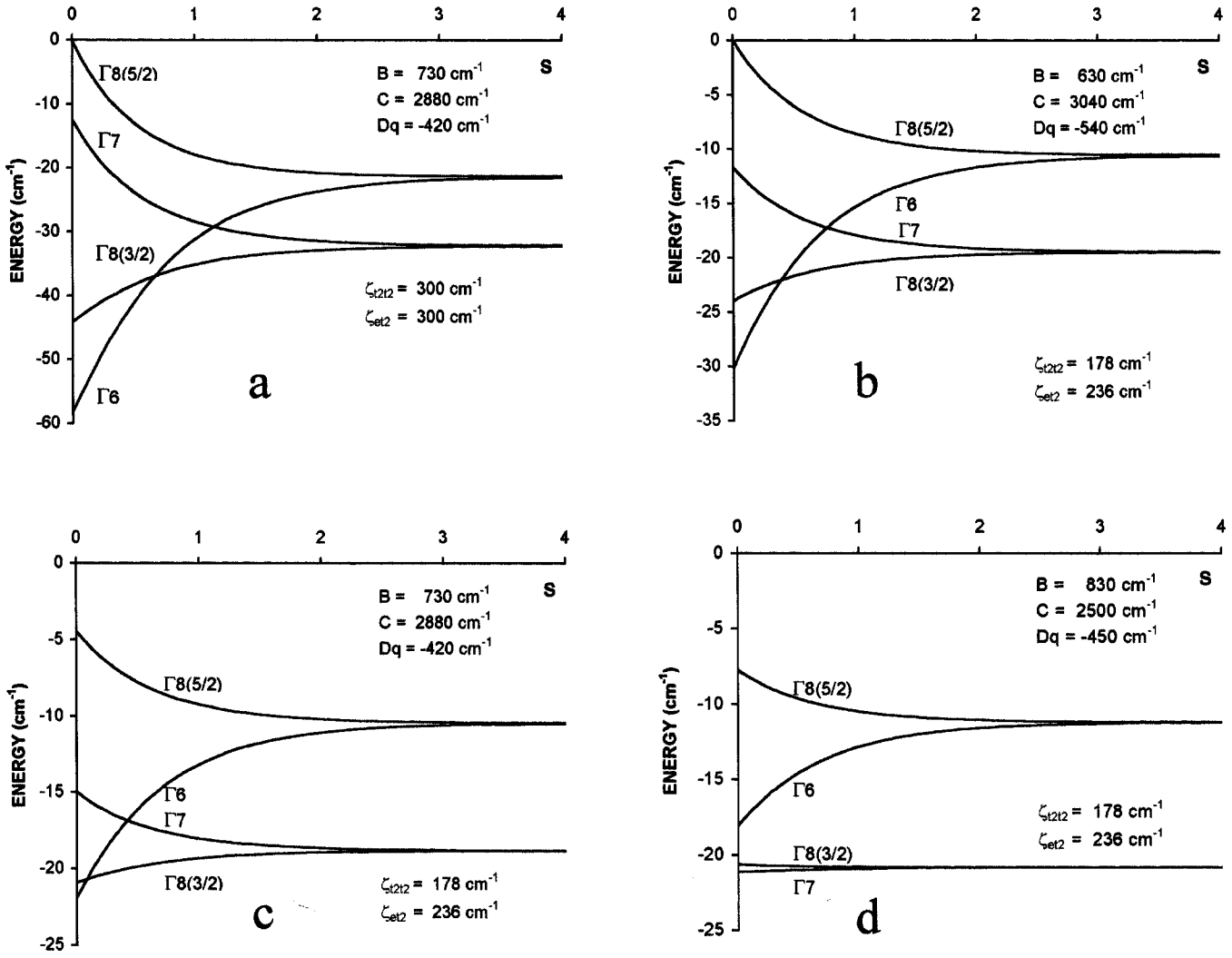

FIG. 1. Theoretical splitting of level $^4T_1(G)$ of Mn in ZnS in terms of the Huang-Rhys factor S, for $\zeta t_2 t_2 = 178$ cm^{-1} and $\zeta e t_2 = 236$ cm^{-1}. (a) gives the energy levels as predicted by the CF model. (b), (c), and (d) correspond to three sets of values for B, C, and Dq. $\hbar\omega_E = 300$ cm^{-1}.

first-order molecular spin-orbit (MSO) splitting of the fluorescent level $^4T_1(G)$ in ZnS is very strongly reduced or even inversed with respect to that predicted by the CF model, and that the first-order MSO splitting of the fluorescent level $^4T_1(G)$ in ZnSe is very large and inversed with respect to that predicted by the CF model.[11]

The aim of this paper is to calculate the second-order MSO interaction which becomes preponderant when the first-order MSO interaction is reduced by vibronic interactions, and to give an overall view of the vibronic structures of orbital triplet levels of d^5 ions in terms of S, by considering the case of the fluorescent level $^4T_1(G)$ of Mn^{2+} in ZnS and ZnSe.

The extended cluster model giving the monoelectronic and multielectronic wave functions for the orbital triplet states, and the first- and second-order MSO interaction, is presented in Sec. II. The vibronic model is presented in Sec. III A. It is shown in Sec. III B that the electronic (and therefore the vibronic) structure of the level $^4T_1(G)$ of Mn^{2+} in ZnS *critcally depends on the second-order MSO interaction.* This is due to the fact that the first-order MSO interaction is very strongly reduced with respect to the value given by the CF model, so that the second-order MSO interaction becomes preponderant. It is shown that, in this case, the vibronic levels strongly depend on the monoelectronic and multielectronic molecular wave functions which govern the MSO interaction.

The electronic and vibronic structures for the level $^4T_1(G)$ of Mn^{2+} in ZnSe are presented in Sec. III C. It is shown that, for this level, *the MSO interaction due to the 4p electrons of the ligands becomes preponderant with respect to the MSO interaction due to the d electrons of the cation.* In this case again, the electronic structure drastically differs from that given by the CF model. In Sec. IV, the experimental results for level $^4T_1(G)$ of Mn^{2+} in ZnS and ZnSe are compared to the theoretical results and a qualitative model is proposed for the structure of the fluorescent levels of Fe^{3+} in InP and GaAs.

II. MSO INTERACTION AND ELECTRONIC STRUCTURE OF LEVELS $^4T_1(G)$ OF Mn IN ZnS AND ZnSe

A. Second-order MSO interaction

The first-order MSO interaction has already been calculated for levels $^4T_1(G)$ of Mn in ZnS and ZnSe (see Ref. 11) by using molecular wave functions which correctly accounted for the orbit lattice coupling constants (OLCC's) of levels $^4T_1(G)$ and $^4T_2(G)$ in ZnS and ZnSe,[13] and for the spin lattice coupling constants (SLCC's) of the fundamental state $^6A_1$ of Mn^{2+} in ZnS, ZnSe, ZnTe, and CdTe.[14] (The OLCC's and SLCC's describe the uniaxial stress effect on excited and fundamental levels, respectively.)

The MSO interaction H_{SOm} is conveniently studied in terms of two matrix elements ζet_1 and $\zeta t_2 t_2$ of the molecular angular momentum. We will now recall the definitions of ζet_2 and $\zeta t_2 t_2$. The operator H_{SOm} describing the MSO interaction is defined in terms of the molecular angular momentum τ_u^i of electron i and in terms of the complex component s_q^i of the spin operators for electron i by[15]

$$H_{SOm}=\sum_q \sum_i \tau_u^i s_q^i,$$

where $u=x$ or y if $q=\pm 1$ and $u=z$ if $q=0$.

Explicitly,

$$\tau_u^i=\zeta_M(r_{iM})\mathbf{I}_{Mu}^i+\zeta_L(r_{iL})\Omega_u^i.$$

Ω^i is the total angular momentum of electron i of the ligands. $\mathbf{I}_{iM}$ and $\mathbf{I}_{iL}$ are one-electron orbital operators for the metal and the ligands respectively. ζ_M and ζ_L are the spin-orbit coupling constants for the cation and the ligands. In the following, the relevant spin-orbit coupling constants will be those of the 3*d* electrons of manganese and of the 3*p* electrons of sulfur and the electrons 4*p* of selenium.

The matrix elements of the molecular spin-orbit interaction can now be expressed in terms of the matrix elements of the operator τ. The relevant matrix elements of τ for the monoelectronic wavefunctions $2e$ and $4t_2$ are

$$\zeta et_2=\frac{i}{2}\langle e\varepsilon|\tau_z|t_2\zeta\rangle$$

and

$$\zeta t_2 t_2=-i\langle t_2\xi|\tau_z|t_2\eta\rangle.$$

Explicitly, ζet_2 and $\zeta t_2 t_2$ are given in terms of the mixing coefficients of the monoelectronic wave functions and of the spin-orbit constants of the metal and of the ligands by

$$\zeta et_2=a^d b^d \zeta_M+[1/(2\sqrt{3})]b^{\pi p}(a^{\pi p}+a^{\sigma p}\sqrt{2})\zeta_L$$

and

$$\zeta t_2 t_2=(a^d a^d-a^p a^p)\zeta_M+a^{\pi p}(a^{\sigma p}\sqrt{2}-a^{\pi p}/2)\zeta_L.$$

The mixing coefficients a and b are defined from the monoelectronic molecular orbitals $4t_2$ and $2e$ of the half-filled shell written in terms of the monoelectronic orbitals of the 3*d* and 4*p* electrons of the cation, and in terms of the orbitals σs, σp, and πp of the ligands as

$$|t_2\gamma\rangle=a^d|dt_2\gamma\rangle+a^p|pt_2\gamma\rangle+a^{\sigma s}|\sigma s t_2\gamma\rangle+a^{\sigma p}|\sigma p t_2\gamma\rangle+a^{\pi p}|\pi p t_2\gamma\rangle,$$

where $\gamma=\xi$, η, or ζ refers to the components of the molecular monoelectronic level $4t_2$, and,

$$|e\gamma'\rangle=b^d|de\gamma'\rangle+b^{\pi p}|\pi p e\gamma'\rangle,$$

where $\gamma'=\theta$ or ε refers to the components of the molecular monoelectronic level $2e$.

As indicated in Sec. I it can be shown here that the CF model is a simple particular case of the molecular model corresponding to $|t_2\gamma\rangle=|dt_2\gamma\rangle$ *and* $|e\gamma'\rangle=|de\gamma'\rangle$, *since in the CF model the d electrons only are considered. Therefore,* $\zeta et_2=\zeta t_2 t_2=\zeta_M$ *and the CF-model is obtained from the molecular model by taking for* ζet_2 *and* $\zeta t_2 t_2$ *the common value of* ζ_M.

All multiplets of the configuration d^5, constructed from the orbitals e and t_2, have been taken into account to calculate the second-order MSO interaction. The 43 multiplets $^2A_1(4)$, $^2A_2(3)$, $^2E(7)$, $^2T_1(8)$, $^2T_2(10)$, $^4E(2)$, $^4A_1(1)$, $^4A_2(1)$, $^4T_1(3)$, $^4T_2(3)$, and $^6A_1(1)$ have been considered. The multiplets are written in the form $^{2S+1}\Gamma(n)$, where S is the total spin, Γ an irreducible representation of the tetrahedral group Td, and n the number of multiplets of the given spin and symmetry. The multielectronic wave functions for the multiplets are obtained by diagonalizing the electrostatic matrix of Sugano, Tanabe, and Kamimura.[16] The diagonalization is performed by using the cubic field parameter Dq and the Racah parameters B and C. For example, the three states $|^4T_1(G)\rangle$, $|^4T_1(P)\rangle$, and $|^4T_1(F)\rangle$ are written in the strong-field scheme as

$$|^4T_{1u}{}^q\rangle=a_1{}^q|^4T_{1u}{}^q(4t_2{}^4 2e)\rangle+a_2{}^q|^4T_{1u}{}^q(4t_2{}^3 2e^2\rangle+a_3{}^q|^4T_{1u}{}^q(4t_2{}^2 2e^3)\rangle,$$

where $q=1$, 2, and 3 refers to the three levels $^4T_1\cdot u=x$, y or z. Then, by considering the spin and orbital degeneracies, we obtained 252 state vectors expressed in terms of Slater determinants constructed from the monoelectronic molecular orbitals $|e\gamma'\rangle$ and $|t_2\gamma\rangle$.

A program has been elaborated to conveniently calculate all relevant matrix elements of the second-order MSO interaction for the multielectronic wave functions. Finally, the electronic energy levels Γ_6 and Γ_7, and the matrix elements for the two Γ_8's are calculated in the spinor group Td^*.

B. Equivalent electronic operator

While the first-order MSO interaction for an orbital triplet level is simply described by an operator in $\boldsymbol{l.S}$ with $\mathbf{l}=1$ and $\mathbf{S}=3/2$, the second-order MSO interaction is much more difficult to handle. Since our aim is to also analyze the vibronic interactions, the electronic energy levels are most conveniently described by the following equivalent operator[17]

$$H_{\rm eq}=c_{T1}\boldsymbol{l}\cdot\boldsymbol{S}+c_E(2/3)(l_\theta S_\theta+l_\varepsilon S_\varepsilon)+c_{A1}(1/3)\boldsymbol{l}^2\boldsymbol{S}^2$$
$$+c_{T2}(1/2)(l_\xi S_\xi+l_\eta S_\eta+l_\zeta S_\zeta),$$

where the index in the c_Γ's means that the operators span the representation Γ of the tetrahedral group Td. It must be noted that the first-order MSO interaction contributes to c_{T1} only, while the second-order MSO interaction contributes to c_{A1}, c_E, c_{T2}, and also to c_{T1}. The term in c_{A1} represents a shift common to the fine structure lines.

The c_Γ's are deduced from the energies of levels Γ_6 and Γ_7, and from the matrix elements for the two Γ_8's by using the following relations

$$W(\Gamma_6)=\tfrac{5}{2}c_{A1}+c_E-\tfrac{5}{2}c_{T1}+\tfrac{3}{2}c_{T2},$$

$$W(\Gamma_7)=\tfrac{5}{2}c_{A1}-c_E+\tfrac{3}{2}c_{T1}+\tfrac{3}{2}c_{T2},$$

$$\langle\Gamma_8(\tfrac{3}{2})|H_{\rm eq}|\Gamma_8(\tfrac{3}{2})\rangle=\tfrac{5}{2}c_{A1}-\tfrac{4}{5}c_E-c_{T1}-\tfrac{6}{5}c_{T2},$$

$$\langle\Gamma_8(\tfrac{5}{2})|H_{\rm eq}|\Gamma_8(\tfrac{5}{2})\rangle=\tfrac{5}{2}c_{A1}+\tfrac{4}{5}c_E+\tfrac{3}{2}c_{T1}-\tfrac{3}{10}c_{T2}.$$

$$\langle\Gamma_8(\tfrac{3}{2})|H_{\rm eq}|\Gamma_8(\tfrac{5}{2})\rangle=\tfrac{3}{5}(c_E-c_{T2}).$$

The contribution to c_{T1} of the first-order MSO interaction and the contributions to c_{T1}, c_E, c_{A1}, and c_{T2} of the second-order MSO interaction can be expressed in terms of ζet_2 and ζt_2t_2 as

$$c_{T1}=\alpha\zeta et_2+\beta\zeta t_2t_2$$

$$c_{\Gamma M\Gamma}=\alpha'_{\Gamma M\Gamma}\zeta et_2{}^2+\beta'_{\Gamma M\Gamma}\zeta t_2t_2{}^2+\gamma'_{\Gamma M\Gamma}\zeta et_2\zeta t_2t_2,$$

where $c_{\Gamma M\Gamma}=c_{T1}$, c_E, c_{A1}, and c_{T2}. These two relations are very convenient to calculate the influence of the ζ's on the energies of the fine structure lines.

C. Electronic structures

In order to have an overall view of the influence of the monoelectronic wave functions on the electronic structures of the fluorescent levels of Mn in ZnS and ZnSe, two sets of monoelectronic wave functions which correctly accounted for the OLCC's (Ref. 13) and SLCC's (Ref. 14) are used for Mn in ZnS and for Mn in ZnSe. Therefore, two sets of values for ζet_2 and ζt_2t_2 are considered in each case.

The influence of the multielectronic wave functions is determined from slightly different sets of values for *B*, *C*, and *Dq* deduced from fittings of the excited energy levels. We will first consider the case of ZnS:Mn.

For the first selected set of monoelectronic wave functions, the interatomic distance is $a=4.41$ a.u., the crystal electric field is $C_{\rm mad}=1.63$, the charge of the lattice is $Q_{\rm lat}=\pm0.8$, the charge of the cation is $Q_M=1.31$ and the theoretical value for the cubic field coefficient is $Dq=-365$ cm^{-1}. The spin-orbit coupling constants are $\zeta_{3d}=301$ cm^{-1} for the electrons *d* of Mn and $\zeta_{3p}=302$ cm^{-1} for the electrons of sulfur. Finally, the molecular model gives $\zeta et_2=236$ cm^{-1} and $\zeta t_2t_2=178$ cm^{-1}. For the second set of monoelectronic wave functions corresponding to $a=4.56$ a.u., $C_{\rm mad}=1.40$, $Q_{\rm lat}=\pm0.8$, $Q_M=0.97$, and $Dq=-419$ cm^{-1}, we obtain $\zeta_{3d}=285$ cm^{-1}, $\zeta_{3p}=308$ cm^{-1}, $\zeta et_2=205$ cm^{-1} and $\zeta t_2t_2=131$ cm^{-1}.

The multielectronic wave functions are obtained from the following values for *B*, *C*, and *Dq*:$B=630$ cm^{-1}, $C=3040$ cm^{-1}, and $Dq=-540$ cm^{-1} (Ref. 18); $B=730$ cm^{-1}, $C=2880$ cm^{-1} and $Dq=-420$ cm^{-1} (Ref. 1); and $B=830$ cm^{-1}, $C=2500$ cm^{-1}, and $Dq=-450$ cm^{-1}. These sets correctly account for the observed excited energy levels of Mn in ZnS.

Tables I(a) and I(b) give the contributions of the first- and second-order MSO interaction to the c's for the level $^4T_1(G)$ of Mn in ZnS for the selected sets of monoelectronic and multielectronic wave functions. In the case of ZnSe:Mn, the first set of monoelectronic wave functions corresponds to $a=4.61$ a.u., $C_{\rm mad}=1.63$, $Q_{\rm lat}=\pm0.7$, $Q_M=1.22$, and $Dq=-310$ cm^{-1}. The spin-orbit coupling constants are $\zeta_{3d}=296$ cm^{-1} for Mn and $\zeta_{4p}=1404$ cm^{-1} for selenium. $\zeta et_2=193.5$ cm^{-1} and $\zeta t_2t_2=-139$ cm^{-1}. The second set corresponds to $a=4.76$ a.u., $C_{\rm mad}=1.33$, $Q_{\rm lat}=\pm0.7$, $Q_M=0.84$, $Dq=-421$ cm^{-1}, $\zeta_{3d}=274$ cm-1, $\zeta_{4p}=1442$ cm^{-1}, $\zeta et_2=150$ cm^{-1}, and $\zeta t_2t_2=-270$ cm^{-1}.

Three sets of values for *B*, *C*, and *Dq* are considered: $B=740$ cm^{-1}, $C=2740$ cm^{-1}, and $Dq=-405$ cm^{-1} (Ref. 19), $B=630$ cm^{-1}, $C=3040$ cm^{-1}, and $Dq=-540$ cm^{-1}; $B=830$ cm^{-1}, $C=2500$ cm^{-1} and $Dq=-450$ cm^{-1}. Since the experimental energy levels are almost identical in ZnS and ZnSe, the second and third sets for *B*, *C*, and *Dq* are chosen to be identical for the two compounds.

Tables I(c) and I(d) give the c's for level $^4T_1(G)$ of Mn in ZnSe for selected sets of wave functions.

A comparison of the *c*'s for ZnS and ZnSe shows that the most striking difference appears for the contribution to c_{T1} of the first-order MSO interaction. As previously shown, this effect is primarily due to the very large contribution of the ligands in the case of ZnSe.

In what concerns the second-order MSO interaction, a somewhat surprising result is that the contributions of this interaction to the *c*'s are not very different for ZnS and ZnSe. This result, which was not evident *a priori*, is due to the fact that in ZnSe, the terms in $\zeta_L{}^2$ are to a large extent compensated by the terms in $\zeta_M\zeta_L$.

For ZnS, the electronic energy levels corresponding to Table I are given in Figs. 1(b)–1(d) and 2(b)–2(d), for $S=0$. For ZnSe, the electronic energy levels corresponding to the second lines of Tables I(c) and I(d) are given in Figs. 3(b) and 3(c)for $S=0$. A more detailed discussion of the electronic and vibronic energy levels will be made in Sec. III.

III. VIBRONIC STRUCTURE FOR LEVELS $^4T_1(G)$ OF Mn^{2+} IN ZnS AND ZnSe

A. Vibronic model

The vibronic interactions can be analyzed from the operator $H_{\rm eq}$ defined in Sec. II by replacing the c_Γ's by coefficients $c_{\Gamma JT}$, defined as follows:

$$c_{T1JT}=c_{T1}e^{-3S/2}-K_1/2,$$

$$c_{EJT}=c_E+K_1+K_2,$$

$$c_{T2JT}=c_{T2}e^{-3S/2}+K_1.$$

TABLE I. Contributions to the c_Γ's of the first- and second-order MSO interaction for the fluorescent levels $^4T_1(G)$ of Mn in ZnS (a,b) and ZnSe (c,d). The results are given for three sets of values for *B*, *C*, and *Dq* and for two sets of values for $\zeta t_2 t_2$ and $\zeta e t_2$. All values are in cm^{-1}.

(a) ZnS:Mn $\zeta t_2 t_2 = 178\ cm^{-1}$ and $\zeta e t_2 = 236\ cm^{-1}$

B	*C*	*Dq*	c_{A1}	c_E	c_{T2}	c_{T1} First order	c_{T1} Second order
630	3040	−540	−5.98	4.48	−1.69	9.01	−2.16
730	2880	−420	−5.84	4.19	−1.29	5.67	−1.85
830	2500	−450	−6.40	4.81	−1.86	4.19	−2.55

(b) ZnS:Mn $\zeta t_2 t_2 = 131\ cm^{-1}$ and $\zeta e t_2 = 205\ cm^{-1}$

B	*C*	*Dq*	c_{A1}	c_E	c_{T2}	c_{T1} First order	c_{T1} Second order
630	3040	−540	−4.29	3.84	−1.49	4.22	−1.52
730	2880	−420	−4.21	3.42	−1.15	1.42	−1.30
830	2500	−450	−4.62	3.89	−1.59	−0.05	−1.81

(c) ZnSe:Mn $\zeta t_2 t_2 = -139\ cm^{-1}$ and $\zeta e t_2 = 193.5\ cm^{-1}$

B	*C*	*Dq*	c_{A1}	c_E	c_{T2}	c_{T1} First order	c_{T1} Second order
630	3040	−540	−3.68	3.73	−1.43	−34.82	−1.14
740	2740	−405	−3.76	3.86	−1.25	−37.15	−0.97
830	2500	−450	−3.83	4.30	−1.65	−39.64	−1.24

(d) ZnSe:Mn $\zeta t_2 t_2 = -270\ cm^{-1}$ and $\zeta e t_2 = 150\ cm^{-1}$

B	*C*	*Dq*	c_{A1}	c_E	c_{T2}	c_{T1} First order	c_{T1} Second order
630	3040	−540	−3.89	0.83	0.48	−50.99	−1.29
740	2740	−405	−3.83	1.18	0.45	−52.30	−1.11
830	2500	−450	−3.71	1.58	0.13	−55.21	−1.20

The terms $K_1$and K_2 are defined by $K_1 = -{\chi_1}^2 f_a/\hbar\omega$, and $K_1 + K_2 = -{\chi_1}^2 f_b/\hbar\omega$, where $f_a = e^{-x}G(x/2)$, with $x = 3E_{JT}/\hbar\omega$, $G(x) = \Sigma x^n/n(n!)$, and $f_b = e^{-x}G(x)$, $S = E_{JT}/\hbar\omega$. E_{JT} is the Jahn-Teller (JT) energy and $\hbar\omega$ is the energy of an effective phonon.

B. Model for the vibronic structure of level $^4T_1(G)$ of Mn in ZnS

The energies, in terms of the Huang-Rhys factor *S*, of the fine-structure lines of level $^4T_1(G)$ of Mn^{2+} in ZnS are given in Fig. 1 a for the CF model and in Figs. 1(b)–1(d) for the molecular model. Figures 1(b)–1(d) give the energy-level schemes for $\zeta t_2 t_2 = 178\ cm^{-1}$ and $\zeta e t_2 = 236\ cm^{-1}$. These figures show that for $S=0$, the overall splitting of 60 cm^{-1} for the CF model [Fig. 1(a)] is reduced to 30 cm^{-1} [Fig. 1(b)], 18 cm^{-1} [Fig. 1(c)] and 15 cm^{-1} [Fig. 1(d)]. We can note that, in Fig. 1(d), the energies of the two levels Γ_7 and $\Gamma_8(\frac{3}{2})$ at lower energy are almost identical and constant.

Figures 2(b), 2(c), and 2(d) give the energies for $\zeta t_2 t_2 = 131\ cm^{-1}$ and $\zeta e t_2 = 205\ cm^{-1}$. We must note the very strong reduction of the overall splitting (15 and 10 cm^{-1} for $S=0$) with respect to the overall splitting (60 cm^{-1} for $S=0$) predicted by the CF model [Fig. 2(a)]. Figures 2(c) and 2(d) show that the ordering of the energy levels Γ_7 and $\Gamma_8(\frac{3}{2})$, on the one hand, and Γ_6 and $\Gamma_8(\frac{5}{2})$, on the other hand, are inverted with respect to the ordering predicted by the CF model. In particular, Figs. 2(c) and 2(d) show that the level Γ_7 is at lower energy and that the level Γ_6 is at higher energy.

These results show that the energies very strongly depend on the second-order MSO interaction whose effect on the energy levels can be of the same order of magnitude or even greater than the first-order MSO interaction. Therefore, *the energy levels are very sensitive both to the values of B, C, and Dq which govern the multielectronic wave functions and to values of $\zeta e t_2$ and $\zeta t_2 t_2$ which depend on the monoelectronic wave functions and on the spin orbit coupling constants of the electrons d of the cation and p of the ligands.*

C. Model for the vibronic structure of level $^4T_1(G)$ of Mn in ZnSe

For level $^4T_1(G)$ of Mn in ZnSe, the energies, in terms *S*, of the fine-structure lines are given in Fig. 3. This figure represents the energy levels for $B = 740\ cm^{-1}$, $C = 2740\ cm^{-1}$, and $Dq = -405\ cm^{-1}$.

Figure 3(b) gives the energy levels as predicted by the molecular model for $\zeta t_2 t_2 = -139\ cm^{-1}$ and $\zeta e t_2 = +193.5\ cm^{-1}$. It must be noted that (i) the overall splitting of 160 cm^{-1} for $S=0$ is much greater than the splitting of 55 cm^{-1} given by the CF model [Fig. 3(a)]; (ii) the level Γ_7 is at lower energy while level Γ_6 is at higher energy whatever the

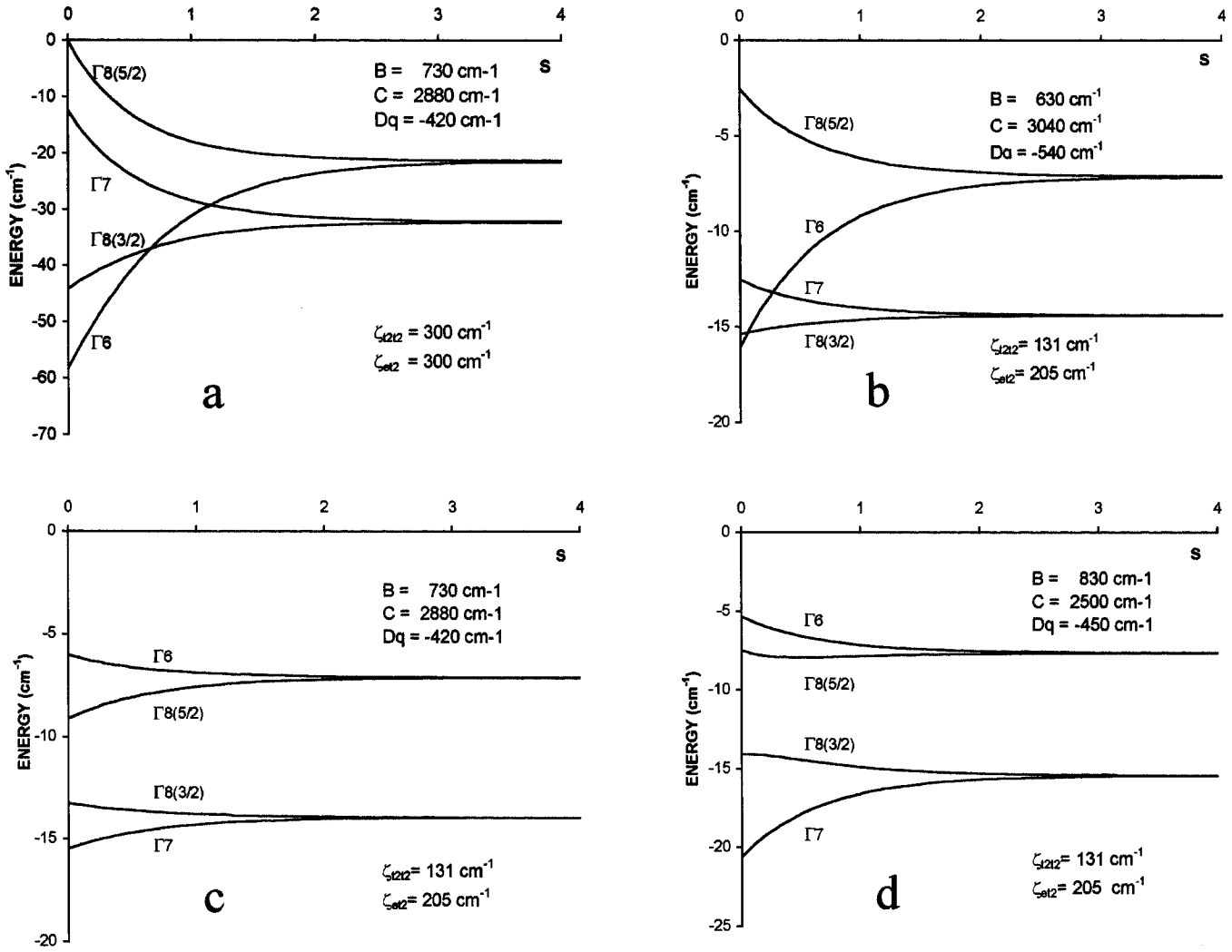

FIG. 2. Theoretical splitting of level $^4T_1(G)$ of Mn in ZnS in terms of the Huang-Rhys factor S, for $\zeta t_2 t_2 = 131$ cm^{-1} and $\zeta e t_2 = 205$ cm^{-1}. As in Fig. 1, (a) gives the energy levels as predicted by the CF model. (b), (c), and (d) correspond to three sets of values for B, C, and Dq. $\hbar\omega_E = 300$ cm^{-1}.

value of S; and (iii) for large values for S, the levels Γ_7 and $\Gamma_8(\frac{5}{2})$ coalesce at lower energy while the levels Γ_6 and $\Gamma_8(\frac{3}{2})$ coalesce at higher energy.

Figure 3(c) gives the energy levels for $\zeta t_2 t_2 = -270$ cm^{-1} and $\zeta e t_2 = 150$ cm^{-1}. We must note that, (i) the overall splitting of 210 cm^{-1} for $S=0$ is four times larger than the splitting predicted by the CF model, and (ii) the ordering of levels Γ_7 and $\Gamma_8(\frac{5}{2})$ at lower energy are inverted with respect to the ordering of Fig. 3(b).

IV. COMPARISON WITH EXPERIMENTS

For Mn^{2+} in ZnS, magnetic-field experiments, performed on crystals of very high quality giving linewidths of 0.6–0.7 cm^{-1}, have unambiguously shown that the level ordering and the energies, with respect to the level at lower energy, of the fine-structure lines of the fluorescent level are $W(\Gamma_7) = 0$, $W[\Gamma_8(\frac{3}{2})] = 0.69$ cm^{-1}, $W[\Gamma_8(\frac{5}{2})] = 9.74$ cm^{-1}, and $W(\Gamma_6) = 10.33$ cm^{-1}.[12] The correct level ordering is obtained in Figs. 2(c) and 2(d). A correct fit of the energy levels is obtained from Fig. 2(c) for $S = 1.2$ or from Fig. 2(d) for $S = 1.4$. The theoretical splittings $W[\Gamma_8(\frac{3}{2})] - W(\Gamma_7) = 0.7$ cm^{-1} and $W(\Gamma_6) - W[\Gamma_8(\frac{5}{2})] = 0.6$ cm^{-1} are in excellent agreement with the experimental values of 0.6 and 0.7 cm^{-1}, respectively, the theoretical energy separation $W[\Gamma_8(\frac{5}{2})] - W[\Gamma_8(\frac{3}{2})]$ between the two groups of lines is of 6.25 cm^{-1} while the experimental value is of 9.04 cm^{-1}. It was shown in Ref. 11 that the experimental and theoretical RDS's are in good agreement.

In the case of ZnSe:Mn, the experimental spectrum reduces to two unresolved lines separated by 11.5 cm^{-1} with relatively large linewidths of 4–5 cm^{-1}.[1] The experimental RDS's are in good agreement with the theoretical values of 9 for the unresolved line at higher energy and 11 for the unresolved line at lower energy.[1] A very good agreement between the experimental and theoretical energy separation and the RDS's is obtained from Fig. 3(c) by taking $S = 1.7$ or from Fig. 3(b) by taking $S > 2.5$. However, it must be noted that, for large values for S, the vibronic model associated with the

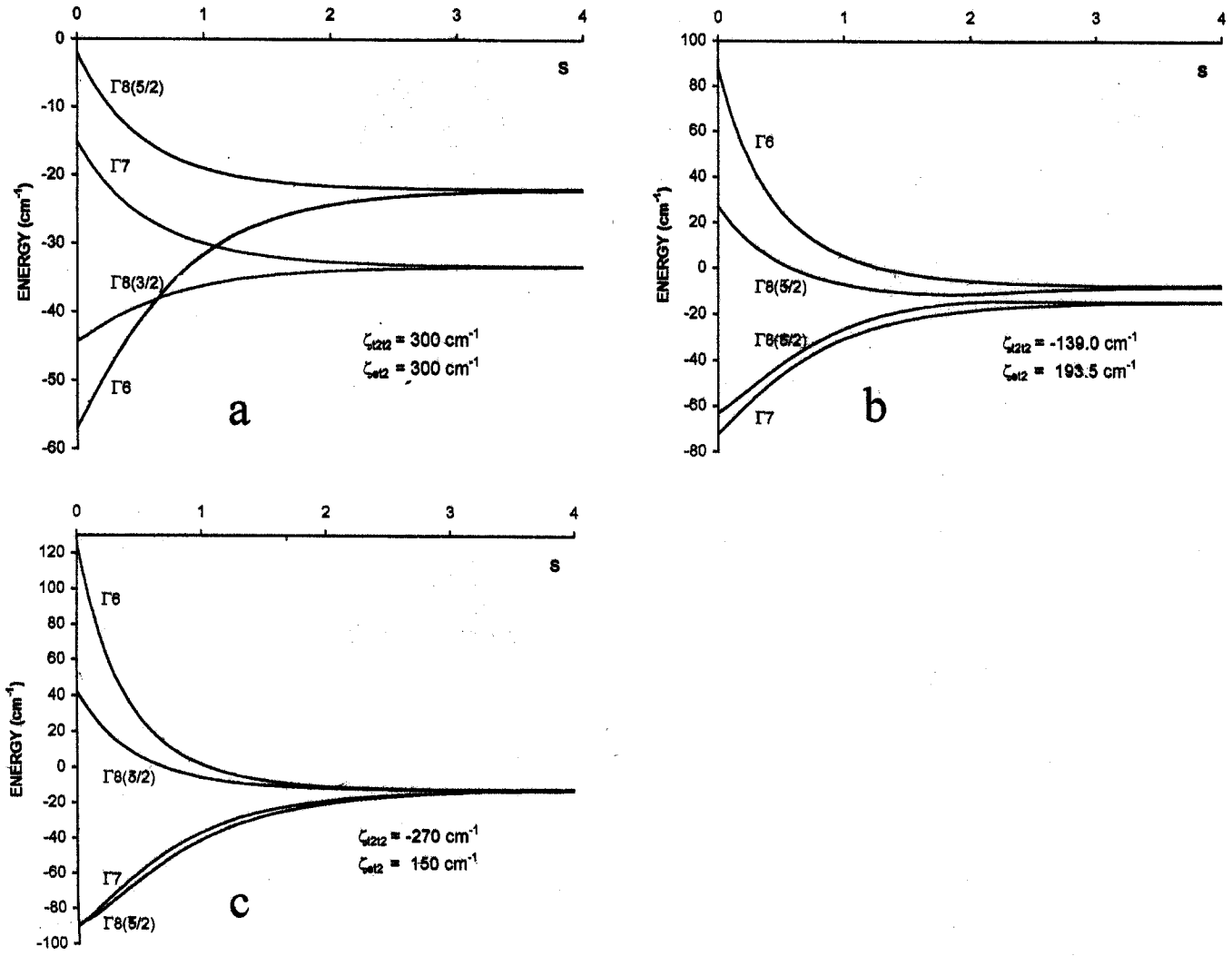

FIG. 3. Theoretical splitting of level ${}^4T_1(G)$ of Mn in ZnSe in terms of the Huang-Rhys factor S, for $B=740$ cm^{-1}, $C=2740$ cm^{-1}. $Dq=-405$ cm^{-1}, and $\hbar\omega_E=240$ cm^{-1}. (a) gives the energy levels as predicted by the CF model. (b) and (c) gives the energy levels for two sets of values for $\zeta t_2 t_2$ and $\zeta e t_2$.

CF model or the covalent model predicts a coalescence of levels associated to the states $|\Gamma_7\rangle$ and $|\Gamma_8'(\frac{3}{2})\rangle = (3/\sqrt{10})|\Gamma_8(\frac{3}{2})\rangle - (1/\sqrt{10})|\Gamma_8(\frac{5}{2})\rangle$ on the one hand and $|\Gamma_6\rangle$ and $|\Gamma_8'(\frac{5}{2})\rangle = (1/\sqrt{10})|\Gamma_8(\frac{3}{2})\rangle + (3/\sqrt{10})|\Gamma_8(\frac{5}{2})\rangle$ on the other hand, so that it is not possible to select one of the two models without having the experimental positions of levels Γ_6 and Γ_7 with respect to levels Γ_8'. Of course, as for Mn^{2+} in ZnS, experimental spectra showing the four fine structure lines could permit to check the validity of the molecular model since the CF model and the molecular model predict different energy-level orderings.

We will now consider the structure of the fluorescent level of Fe^{3+} in InP and GaAs and give indications concerning the interpretation following the molecular model. In the case of Fe^{3+} in InP, the emission spectra were studied by Pressel *et al.*,[9] the uniaxial stress effect and the Zeeman effect were studied in Ref. 7. It must be noted that in emission spectra, the levels are thermally populated so that the amplitudes of the lines as well as the linewidths depend on temperature, thus complicating the interpretation of the measurements, in particular those of the RDS's. The spectrum consists of two sharp lines (linewidths of 0.26 cm^{-1}) separated by 4.14 cm^{-1} and a broader line (linewidth of 2 cm^{-1}) appearing at 22 cm^{-1}.[9] The two lines at lower energy have been associated with levels Γ_7 for the line at lower energy and Γ_8 for the line at 4.14 cm^{-1}; the broad line at 22 cm^{-1} has been associated with levels Γ_6 and Γ_8, the coupling being to ε modes only.[7] It is possible to propose for InP:Fe a molecular model similar to that developed for ZnS:Mn since the spin-orbit coupling constants of the electrons of the ligands and of the cation are not very different ($\zeta_L=217$ cm^{-1} for an effective charge of -1 for phosphorus in InP, $\zeta_L=298$ cm^{-1} for an effective charge of -1 for sulfur in ZnS, $\zeta_{Fe}=426$ cm^{-1} for an effective charge of $+2$, and $\zeta_{Mn}=286$ cm^{-1} for an effective charge of $+1$). Energy level schemes similar to those of Fig. 2(c) or 2(d) could account for the energy level scheme in InP.

In the case of Fe^{3+} in GaAs, uniaxial stress experiments and Zeeman experiments performed at low temperature on

the level at lower energy have shown that this level is an orbital singlet Γ_7 coupled to ε modes; the next level at 6 cm^{-1} is a level Γ_8, another level at 12.6 cm^{-1} has been observed in emission spectra, and a level at 21 cm^{-1} has been predicted from a fitting of the Zeeman experiments.[5,7] The molecular model developed for ZnSe:Mn seems to be adaptable, since the spin-orbit constants of the electrons of the ligands are very large (for example, $\zeta_L = 984$ cm^{-1} for an effective charge of -1 for arsenium in GaAs and $\zeta_L = 1442$ cm^{-1} for Se in ZnSe). An energy level scheme similar to that of Fig. 3(b) could account for the fine structure of the fluorescent level of Fe^{3+} in GaAs by taking $1.4 < S < 2$. For Fe^{3+} in ZnS, ZnO, and GaN considered in Sec. I, it is not possible to suggest a model from the published emission spectra without complementary studies of the uniaxial stress effect and/or the Zeeman effect.

V. CONCLUSION

A complete molecular model involving the second-order MSO interaction has been elaborated and several characteristic energy-level schemes have been presented in order to show the importance and the complexity of covalency effects on the fluorescent levels of d^5 ions. For convenience, the results have been compared to those given by the well known CF model.

Concerning the influence of the monoelectronic wave functions and of the spin-orbit coupling constants of the electrons of the cation and of the ligands on the first-order MSO interaction, it has been shown that, in the case of ZnS, the first-order MSO interaction is strongly reduced with respect to the value predicted by the CF model. This is due to the fact that the contributions of the electrons of the cation and of the ligands are of opposite sign and that the spin-orbit constants ζ_M and ζ_L are almost identical. In that case, the second-order MSO interaction becomes preponderant to describe the electronic levels. No such compensation exists in the case of ZnSe, because ζ_L is approximately four times greater than ζ_M, so that the influence of the ligands becomes preponderant and the electronic energy levels are inverted with respect to the energy levels predicted by the CF model. Furthermore, the overall splitting of the electronic levels is four times greater than that predicted by the CF model. In this case, the diagonal second-order MSO interaction becomes important as soon as the first-order MSO interaction is reduced by vibronic interaction.

It has been shown that, for the second-order MSO interaction, the influence of the ligands are not very different in ZnS and ZnSe although the spin-orbit coupling constants of the electrons of the ligands are approximately four times larger in ZnSe than in ZnS. This means that, for Mn in ZnSe, the term in ζ_L^2 is partly compensated for by the terms in $\zeta_L \zeta_M$. Concerning the multielectronic wave functions, it has been shown that, for ZnS, the MSO interaction is very sensitive to the values for *B*, *C*, and *Dq* and that the ordering of the vibronic energy levels strongly depends on these parameters.

Finally, the four lines of the vibronic structure of the fluorescent level of Mn^{2+} in ZnS have been interpreted from the molecular model. A quantitative model has been proposed for the two observed vibronic lines of the fluorescent level of Mn^{2+} in ZnSe, and crude models have been proposed for the unexpected vibronic structures of the fluorescent levels of Fe^{3+} in InP and GaAs.

ACKNOWLEDGMENTS

Thanks are due to F. S. Ham, B. Kaufmann, and A. Dörnen for very helpful discussions concerning Fe^{3+} in InP and GaAs.

[1] R. Parrot, C. Naud, C. Porte, D. Fournier, A. C. Boccara, and J. C. Rivoal, Phys. Rev. B **17**, 1057 (1978).
[2] G. Hofmann, F. G. Anderson, and J. Weber, Phys. Rev. B **43**, 9711 (1991).
[3] A. Hoffmann, R. Heitz, and I. Broser, Phys. Rev. B **41**, 5806 (1990).
[4] R. Heitz, A. Hoffmann, and I. Broser, Phys. Rev. B **45**, 8977 (1992).
[5] K. Pressel, G. Bohnert, G. Rückert, A. Dörnen, and K. Thonke, J. Appl. Phys. **71**, 5703 (1992).
[6] K. Pressel, G. Rückert, A. Dörnen, and K. Thonke, Phys. Rev. B **46**, 13 171 (1992).
[7] B. Kaufmann, A. Dörnen, and F. S. Ham, in *Proceedings of the 23rd International Conference on the Physics of Semiconductors, Berlin, Germany, 21-26 July 1996*, edited by M. Scheffler and R. Zimmermann (World Scientific, Singapore, 1996), Vol. 4, p. 2829.
[8] J. Baur, K. Kaier, M. Kunzer, U. Kaufmann, J. Schneider, H. Amano, I. Akasaki, T. Detchprohm, and K. Hiramatsu, Appl. Phys. Lett. **64**, 857 (1994); R. Heitz, P. Thurian, I. Loa, L. Eckey, A. Hoffmann, I. Broser, K. Pressel, B. K. Meyer, and E. N. Mokhov, *ibid.* **67**, 2822 (1995).
[9] K. Pressel, G. Bohnert, A. Dörnen, B. Kaufmann, J. Denzel, and K. Thonke, Phys. Rev. B **47**, 9411 (1993).
[10] P. Koidl, Phys. Status Solidi B **74**, 477 (1976).
[11] R. Parrot, D. Boulanger, M. N. Diarra, U. W. Pohl, B. Litzenburger, and H. E. Gumlich, Phys. Rev. B **54**, 1662 (1996).
[12] D. Boulanger, R. Parrot, M. N. Diarra, U. W. Pohl, B. Litzenburger, and H. E. Gumlich, Phys. Rev. B **58**, 12 567 (1998).
[13] D. Boulanger and R. Parrot, J. Chem. Phys. **17**, 1469 (1987).
[14] R. Parrot and D. Boulanger, Phys. Rev. B **47**, 1849 (1993).
[15] A. A. Misetich and T. Buch, J. Chem. Phys. **42**, 2524 (1964).
[16] S. Sugano, Y. Tanabe, and H. Kamimura, in *Multiplets of Transition Metal Ions in Crystals* (Academic, New York, 1970).
[17] F. S. Ham, Phys. Rev. **138**, 1727 (1965); F. S. Ham, in *Electron Paramagnetic Resonance*, edited by S. Geschwind (Plenum, New York, 1972).
[18] R. Parrot, C. Naud, D. Curie, U. Pohl, W. Busse, and H. E. Gumlich, J. Lumin. **31/32**, 293 (1984).
[19] D. Langer and H. J. Richter, Phys. Rev. **146**, 554 (1966).